IEEE Photonics Journal
An IEEE Photonics Society Publication

Open Access

Generating in-Plane Optical Orbital Angular Momentum Beams With Silicon Waveguides

Volume 5, Number 2, April 2013

Dengke Zhang
Xue Feng
Kaiyu Cui
Fang Liu
Yidong Huang, Member, IEEE

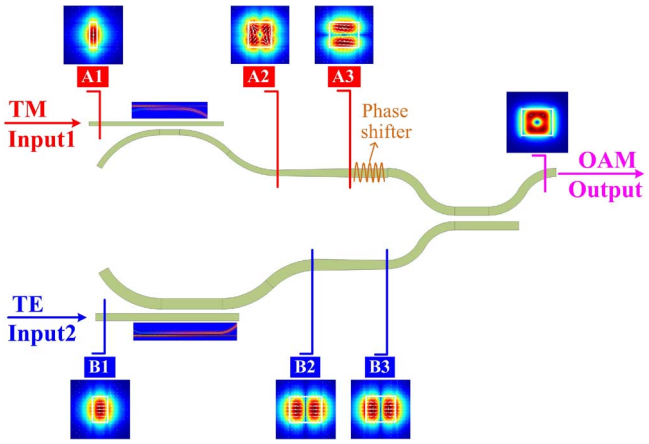

DOI: 10.1109/JPHOT.2013.2256888
1943-0655/$31.00 ©2013 IEEE

IEEE photonics SOCIETY

IEEE

Generating in-Plane Optical Orbital Angular Momentum Beams With Silicon Waveguides

Dengke Zhang, Xue Feng, Kaiyu Cui, Fang Liu, and Yidong Huang, *Member, IEEE*

Department of Electronic Engineering, Tsinghua National Laboratory for Information Science and Technology, Tsinghua University, Beijing 100084, China

DOI: 10.1109/JPHOT.2013.2256888
1943-0655/$31.00 ©2013 IEEE

Manuscript received March 12, 2013; revised March 27, 2013; accepted March 28, 2013. Date of publication April 4, 2013; date of current version April 12, 2013. This work was supported in part by the National Basic Research Program of China under Grants 2011CBA00608 and 2011CBA00303 and in part by the National Natural Science Foundation of China under Grants 61036011 and 61036010. Corresponding author: X. Feng (e-mail: x-feng@tsinghua.edu.cn).

Abstract: A simple on-chip integrated structure is proposed to generate optical orbital angular momentum (OAM) beams, where only silicon waveguides and couplers are involved. The operating principle is based on mode converting and proper controlling the phase shift of second-order propagating mode so that OAM modes with charge numbers of 1 or -1 can be selectively generated with mode purity $> 90\%$. The proposed device is very compact with footprint of $< 120\ \mu\text{m} \times 50\ \mu\text{m}$ and can be easily fabricated with CMOS technology. Thus, such OAM mode generator is a promising candidate for applications ranging from optical tweezers and optical spanners to optical communications.

Index Terms: Optical orbital angular momentum (OAM), integrated optical devices.

1. Introduction

An optical beam with orbital angular momentum (OAM) has a helical wavefront, meaning that the phase of electric vector field has an $l\theta$ dependence where l is an integer and θ is the azimuthal angle. For such an optical beam, the value of OAM per photon is $l\hbar$ and l is referred to as topological charge number [1]. The OAM modes with different charge numbers, which can be any integer from $-\infty$ to ∞, are orthogonal to each other. Owing to such unique characteristics, OAM beams have inspired significant interest in various fields, including optical tweezers and spanners, imaging, communications, and quantum entanglement [2]–[6]. For each application, efficiently generating OAM beams is always required. Traditionally, there are several proposed approaches, such as diffractive optical devices, holograms, phase plates, or spatial light modulators [7]. Recently, integrated approaches based on fibers or silicon devices are developed due to their outstanding features of small footprint, lightweight, low-cost, and adaptation for various applications [8]–[14]. And these OAM generators can be divided into two groups; one is that OAM beams are generated out-plane and propagated in free space [8]–[11], and the other is that OAM beams are generated in-plane and propagated in waveguides [12]–[14]. For the latter, it attracts a lot of attentions to fully exploiting the unique feature of OAM beams in the region of guided optics. However, most of these reported integrated OAM generators require very highly critical dimension (such as dimension of coupling gaps between waveguides) control technology to ensure uniform spatial distributions of multicoupled waveguides [13], [14]. And OAM beams is generated in-plane on a silicon chip has not been reported. Thus, an integrated and easily fabricated OAM generator in-plane is also in great demand.

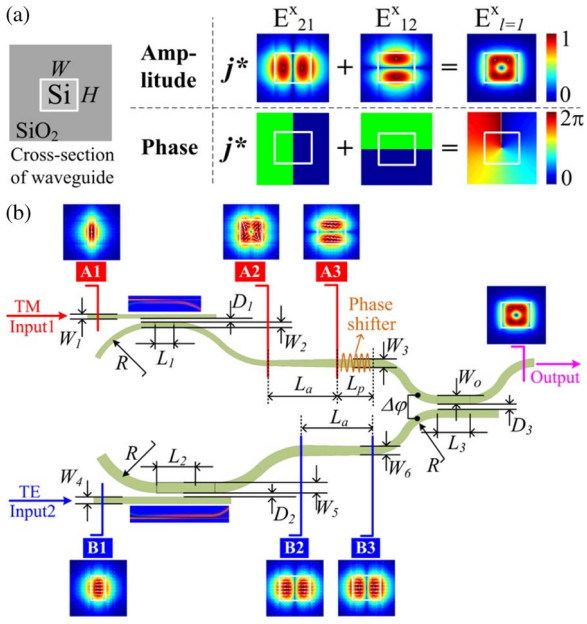

Fig. 1. (a) Cross section of silicon waveguide, and amplitude and phase evolutions of generation of OAM mode in this waveguide; (b) The whole schematic structure for generation of OAM beams and evaluation of generation of OAM beams (Media1-3).

In this paper, we propose and demonstrate a feasible approach to generate OAM beams on a silicon-on-insulator (SOI) chip, while the footprint is as small as $< 120\ \mu\text{m} \times 50\ \mu\text{m}$. The whole structure is simply constructed by coplanar integrated elements of silicon waveguides and couplers. Through two coherent inputs of TE and TM modes, two fundamental modes are initially excited and then transformed to second-order modes through directional couplers. After adiabatic conversion, such two second-order modes are combined by a coupler at the end to generate OAM beams in succession. By adjusting phase shift of one of the second-order modes, charge numbers of 1 or -1 can be selected and the purity of generated OAM modes can exceed 90%. What is more, such an OAM generator can be easily fabricated by the CMOS technology; thus, we believe such an integrated and compact OAM mode generator would be usable for a wide range of applications, such as optical tweezers, optical spanners, and optical communications.

2. Principle and Structure

As shown by Allen *et al.*, a helically phased Laguerre–Gaussian mode LG_{01} ($l = 1$ or -1) could be obtained by combining two high-order Hermite–Gaussian modes of HG_{01} and HG_{10} [1]. Along this way, with a well-designed silicon rectangular waveguide, in which high-order modes could propagate, OAM mode with $l = 1$ or -1 also can be generated by coherent superposition between second-order modes of E^x_{21} and E^x_{12} with a phase difference of $\pi/2$ or $-\pi/2$. Fig. 1(a) illustrates this concept and demonstrates the evolutions of amplitude and phase of the electromagnetic fields. The generated OAM eigenmode can be expressed as $E^x_{l=1} = jE^x_{21} + E^x_{12}$. Thus, multimode Si-waveguide could be employed for OAM generation. However, there are still two main obstacles. One is achieving of phase matching between such two combined modes, and the other is how to excite second-order modes. For phase matching, two degenerate modes (with the same propagation constant) are required, which can be achieved by carefully designing the Si-waveguide. The difficulty of exciting second-order modes comes from inefficient coupling between the modes in Si-waveguides and that from the output of the integrated single-mode lasers, single-mode fiber (SMF) pigtailed lasers, or multimode lasers. Actually, the two fundamental modes of E^x_{11} (TE-like) and E^y_{11} (TM-like) in Si-waveguide can be easily excited by the output of SMF pigtailed lasers or integrated

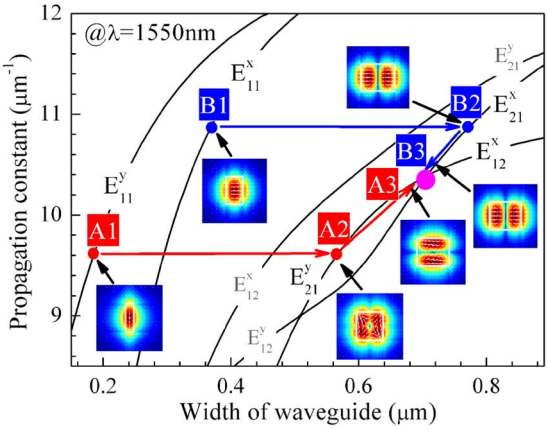

Fig. 2. Structure dispersion relationship about propagation constant and width of silicon waveguide at height of 600 nm.

single-mode lasers if the polarization state is well controlled. So an effective method to obtain second-order modes is through mode converting from fundamental modes, which can be achieved by adopting directional couplers. However, if second-order modes are directly transformed from fundamental modes, both of E_{21}^x and E_{12}^x would be obtained simultaneously, which would make it more difficult to achieve required phase shift between them. Thus, coupling crosstalk would be significant, and the purity of generated OAM beams would be deteriorated. In order to improve the mode purity, we thus propose a two-path and two-step design. The desired modes of E_{21}^x and E_{12}^x are generated in two separated paths, and each path is formed by a two-step mode conversion. The first step is that, with directional couplers, modes of E_{11}^x and E_{11}^y are coupled to two intermediate modes, which are different from the desired modes of E_{21}^x and E_{12}^x in terms of mode distribution and propagation constant. Then, such two intermediate modes are converted to E_{21}^x and E_{12}^x with adiabatic converting waveguides, respectively. At last, E_{21}^x and E_{12}^x are combined by a coupler to generate OAM beam. The whole mode converting process along with our proposed structure is depicted in Fig. 1(b).

Considering the feasibility of fabrication, all waveguides are required to be coplanar with equal height so that the width of waveguide is the only parameter to control propagating mode. Thus, in our simulation, the height of Si-waveguide is fixed as 600 nm and then design the proper width for fundamental, intermediate, and eventual second-order modes, respectively. The dispersion relations with varied waveguide width (W) are calculated at the wavelength of 1550 nm by finite-element method, as shown in Fig. 2. The refractive indexes of silicon core/silicon dioxide cladding are set as 3.45/1.46. Clearly, the desired modes of E_{21}^x and E_{12}^x can be sustained at wider width, and there is a crossing point (marked by a pink point) at $W = 707$ nm, where they are degenerate. Thus, if mode E_{12}^x and E_{21}^x are combined in a Si-waveguide with W of $\sim$707 nm (marked as A3 and B3), an OAM mode can be generated. And with narrower waveguide width, only the fundamental modes of E_{11}^x and E_{11}^y exist. In our proposed approach, the second-order modes are obtained by the transformation of fundamental modes; thus, two proper paths could be designed from the dispersion curves.

For obtaining desired mode of E_{12}^x, E_{11}^y mode is first coupled to the intermediate E_{21}^y mode using a coupler, and in this step, the wave-vector matching should be met for the optimum transformation; thus, path A1 $\rightarrow$ A2 (marked in Fig. 2) is selected corresponding to the same propagation constant of two modes. Then, the intermediate E_{21}^y mode is adiabatically converted to E_{12}^x by slowly varied waveguide width, which is denoted as A2 $\rightarrow$ A3 in Fig. 2. Similarly, for E_{21}^x, the transforming path is expressed as $E_{11}^x \rightarrow E_{21}^x \rightarrow E_{21}^x$ (marked as B1 $\rightarrow$ B2 $\rightarrow$ B3 in Fig. 2). Such two paths are also marked in Fig. 1(b). At output end, there is a coupler to combine E_{12}^x and E_{21}^x, as well as to generate the OAM beams. Obviously, the charge number could be varied as $l = 1$ or -1 if the phase

TABLE 1
Values of structure parameters for generation of OAM beams

			Arm1 (A1→A2→A3)						Arm2 (B1→B2→B3)					Coupler at end		
H (nm)	R (μm)	L_a (μm)	D_1 (nm)	L_1 (μm)	W_1 (nm)	W_2 (nm)	W_3 (nm)	L_p (μm)	D_2 (nm)	L_2 (μm)	W_4 (nm)	W_5 (nm)	W_6 (nm)	D_3 (nm)	L_3 (μm)	W_o (nm)
600	10	30	250	8	180	560	707	7	200	25	360	760	707	100	7	707

difference between the two optical path $(\Delta\varphi)$ is properly set as $\pi/2$ or $-\pi/2$, which can be easily achieved by inserting a tunable phase shifter with the aid of thermo-optic effect of silicon [15]. Here, we assume that the phase shifter is inserted in the path of A1 → A2 → A3 [see Fig. 1(b)].

3. Simulation Results and Analyses

In our simulation, the values of structure parameters are determined as follows. For the modes of E_{12}^x and E_{21}^x, and the generated OAM mode, W_3, W_6, and W_o are all set as 707 nm. For intermediate modes, W_2 and W_5 are relatively optional and selected as 560 nm and 760 nm in this paper. Once W_2 and W_5 are selected, W_1 and W_4 can be determined with the wave-vector matching condition, which could be obtained from dispersion curves (see Fig. 2). Here, they are 180 nm and 360 nm, respectively. Once the width of each waveguide is determined, other structure parameters marked in Fig. 1(b) can be optimized to achieve well mode couplings with finite-difference time-domain (FDTD) method. Specially, for the phase shifter, this could be realized by tuning silicon refractive index of waveguide with thermal tuning method and the tuned variation of silicon refractive index could be larger than 0.05 [16]. To realize the switch between OAM state of $l = 1$ and $l = -1$, the required phase change of phase shifter is π (from $-\pi/2$ to $\pi/2$). Here, we set the variation of silicon refractive index is 0.04, and then, the required length of waveguide [marked as L_p in Fig. 1(b)] is 17 μm. All the values of structure parameters are summarized in Table 1. With such designed structure, OAM mode of $l = 1$ or -1 are generated at $\Delta\varphi = \pi/2$ or $-\pi/2$, and the mode evolutions are also shown in Fig. 1(b) and Media1-3. Meanwhile, the efficiency of mode conversion for each stage is summarized in Fig. 3(a).

To evaluate the mode purity of generated OAM, the normalized power weight coefficient is calculated [14], [17]

$$C_l = \iint F(x,y)\psi_l^*(x,y)dxdy \quad \sum_l |C_l|^2 = 1 \tag{1}$$

where $F(x,y)$ is the electrical field distribution of the generated OAM beam in the silicon waveguide, and $\psi_l(x,y)$ is that of lth order OAM eigenmode in the same waveguide. Fig. 3(b) shows the calculated charge weights (CWs). It clearly shows that the mode purity is higher than 90% for $l = 1$ or -1, that is, extinction ratio (ER) between the mode of $l = 1$ (or -1) and $l = 0$ is higher than 10 dB. Meanwhile, total insertion loss (IL) is only -0.70 dB.

To investigate fabrication tolerance, the impact of fluctuated value of structure parameters on the ER and IL is also considered. As shown in Fig. 1(b), the key structure parameters are the gap width (D_i) between coupling waveguides, waveguide width (W_i), and coupler length (L_i). For more clarity and simplicity, only results for $l = 1$ $(\Delta\varphi = \pi/2)$ are shown. Fig. 4(a)–(c) shows the calculated ER and IL versus the offset of D_i, W_i, and L_i, respectively. From them, we can find that ER is more sensitive for negative offset of gap and IL is more sensitive for negative offset of waveguide width so that such two parameters should be pay more attention in practical fabrication. Furthermore, the tolerance of ER and IL is also investigated with varied phase shift $(\Delta\varphi)$. Fig. 4(d) shows that fluctuation of $\Delta\varphi$ could be ignored with precision voltage control of IC for thermal tuning. The results for OAM mode of $l = -1$ are similar. From all discussed above, the proposed structure is with

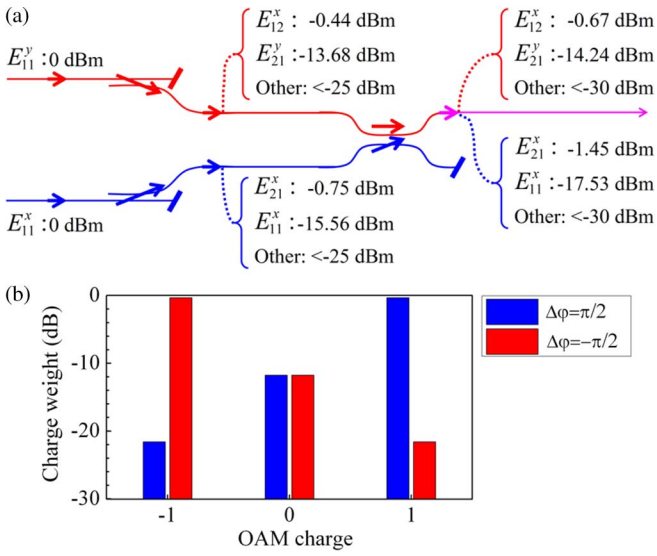

Fig. 3. (a) Conversion efficiencies of modes at each stage. (b) CW of the generated OAM beams.

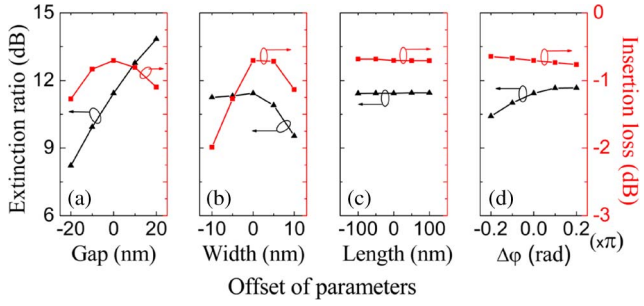

Fig. 4. Dependence of ER and IL on the offset of (a) gap between coupling waveguides, (b) width of waveguides, (c) length of couplers, and (d) the phase shift induced by phase shifter.

strong robustness. Thus, based on the existing mature CMOS technology (typical critical dimension control of about 3 nm of 32-nm node technology), our proposed approach for integrated OAM generator is very feasible and efficient.

In the aforementioned part, we presented the approach for generation OAM beams in Si waveguides with mode superposition, and proposed a simple device design for generating OAM modes of $l = 1$ or -1. It should be mentioned that it is hard to apply the proposed structure on generating higher order OAM modes since higher order modes are needed while not supported in the Si waveguide adopted in this work [18]. However, if higher order modes can be generated in Si waveguides, higher order OAM modes can be obtained following the same method shown in this paper. One possible solution is adopting Si waveguides with larger size of cross section, and the couplers should be carefully designed according to the waveguide. Alternatively, integrated transformation optics as amazing tool may be helpful for achieving mode conversions between fundamental modes and higher order modes [19]–[21].

4. Conclusion

In this paper, a dynamic and integrated OAM beams generator on a SOI chip has been proposed and demonstrated with numerical simulation. The charge number of OAM mode can be controlled by the phase shifter, while the mode purity can be as high as 93% (ER of 11.4 dB) and the IL is only

−0.70 dB. Due to the merits of in-plane, compactness, fabricating feasibility, and stability, we believe that such an integrated OAM beam generator is very potential for application of optical tweezers, optical spanners, and optical communications. Particularly, the in-plane generated OAM beams will bring new prospect for manipulation and transportation of nano particles.

References

[1] L. Allen, M. Beijersbergen, R. Spreeuw, and J. Woerdman, "Orbital angular momentum of light and the transformation of Laguerre–Gaussian laser modes," *Phys. Rev. A*, vol. 45, no. 11, pp. 8185–8189, Jun. 1992.

[2] N. B. Simpson, L. Allen, and M. J. Padgett, "Optical tweezers and optical spanners with Laguerre–Gaussian modes," *J. Mod. Opt.*, vol. 43, no. 12, pp. 2485–2492, Dec. 1996.

[3] S. Fürhapter, A. Jesacher, S. Bernet, and M. Ritsch-Marte, "Spiral phase contrast imaging in microscopy," *Opt. Exp.*, vol. 13, no. 3, pp. 689–694, Feb. 2005.

[4] J. Wang, J.-Y. Yang, I. M. Fazal, N. Ahmed, Y. Yan, H. Huang, Y. Ren, Y. Yue, S. Dolinar, M. Tur, and A. E. Willner, "Terabit free-space data transmission employing orbital angular momentum multiplexing," *Nat. Photon.*, vol. 6, no. 7, pp. 488–496, Jun. 2012.

[5] F. Tamburini, E. Mari, A. Sponselli, B. Thidé, B. Thidé, A. Bianchini, A. Bianchini, and F. Romanato, "Encoding many channels on the same frequency through radio vorticity: First experimental test," *New J. Phys.*, vol. 14, no. 3, pp. 033001-1–033001-17, Mar. 2012.

[6] A. Mair, A. Vaziri, G. Weihs, and A. Zeilinger, "Entanglement of the orbital angular momentum states of photons," *Nature*, vol. 412, no. 6844, pp. 313–316, Jul. 2001.

[7] M. Yao and M. J. Padgett, "Orbital angular momentum: Origins, behavior and applications," *Adv. Opt. Photon.*, vol. 3, no. 2, pp. 161–204, Jun. 2011.

[8] N. K. Fontaine, C. R. Doerr, and L. Buhl, "Efficient multiplexing and demultiplexing of free-space orbital angular momentum using photonic integrated circuits," in *Proc. Opt. Fiber Commun. Conf.*, 2012, pp. 1–3.

[9] T. Su, R. P. Scott, S. S. Djordjevic, N. K. Fontaine, D. J. Geisler, X. Cai, and S. J. B. Yoo, "Demonstration of free space coherent optical communication using integrated silicon photonic orbital angular momentum devices," *Opt. Exp.*, vol. 20, no. 9, pp. 9396–9402, Apr. 2012.

[10] X. Cai, J. Wang, M. Strain, B. Johnson-Morris, J. Zhu, M. Sore, J. L. OBrien, M. G. Thompson, and S. Yu, "Integrated compact optical vortex beam emitters," *Science*, vol. 338, no. 6105, pp. 363–366, Oct. 2012.

[11] D. Zhang, X. Feng, and Y. Huang, "Encoding and decoding of orbital angular momentum for wireless optical interconnects on chip," *Opt. Exp.*, vol. 20, no. 24, pp. 26986–26995, Nov. 2012.

[12] Y. Yan, L. Zhang, J. Wang, J.-Y. Yang, I. M. Fazal, N. Ahmed, A. E. Willner, and S. J. Dolinar, "Fiber structure to convert a Gaussian beam to higher-order optical orbital angular momentum modes," *Opt. Lett.*, vol. 37, no. 16, pp. 3294–3296, Aug. 2012.

[13] Y. Yan, J. Wang, L. Zhang, J.-Y. Yang, I. M. Fazal, N. Ahmed, B. Shamee, A. E. Willner, K. Birnbaum, and S. Dolinar, "Fiber coupler for generating orbital angular momentum modes," *Opt. Lett.*, vol. 36, no. 21, pp. 4269–4271, Nov. 2011.

[14] Y. Yan, Y. Yue, H. Huang, J.-Y. Yang, M. R. Chitgarha, N. Ahmed, M. Tur, S. J. Dolinar, and A. E. Willner, "Efficient generation and multiplexing of optical orbital angular momentum modes in a ring fiber by using multiple coherent inputs," *Opt. Lett.*, vol. 37, no. 17, pp. 3645–3647, Sep. 2012.

[15] F. Gan, T. Barwicz, M. Popovic, M. S. Dahlem, C. W. Holzwarth, P. T. Rakich, H. I. Smith, E. P. Ippen, and F. X. Kartner, "Maximizing the thermo-optic tuning range of silicon photonic structures," in *Proc. Photon. Switch.*, 2007, pp. 67–68.

[16] A. Kaiyu, F. Xue, H. Yidong, Z. Qiang, Z. Huang, and Z. Wei, "Broadband switching functionality based on defect mode coupling in W2 photonic crystal waveguide," *Appl. Phys. Lett.*, vol. 101, no. 15, pp. 151110-1–151110-4, Oct. 2012.

[17] G. Molina-Terriza, J. P. Torres, and L. Torner, "Management of the angular momentum of light: Preparation of photons in multidimensional vector states of angular momentum," *Phys. Rev. Lett.*, vol. 88, no. 1, pp. 013601-1–013601-4, Jan. 2002.

[18] M. Padgett, J. Courtial, and L. Allen, "Light's orbital angular momentum," *Phys. Today*, vol. 57, no. 5, pp. 35–40, May 2004.

[19] J. Pendry, D. Schurig, and D. Smith, "Controlling electromagnetic fields," *Science*, vol. 312, no. 5781, pp. 1780–1782, Jun. 2006.

[20] U. Leonhardt, "Optical conformal mapping," *Science*, vol. 312, no. 5781, pp. 1777–1780, Jun. 2006.

[21] H. Chen, C. Chan, and P. Sheng, "Transformation optics and metamaterials," *Nat. Mater.*, vol. 9, no. 5, pp. 387–396, May 2010.